Article

Cell Reports

Independent Stem Cell Lineages Regulate Adipose Organogenesis and Adipose Homeostasis

Graphical Abstract

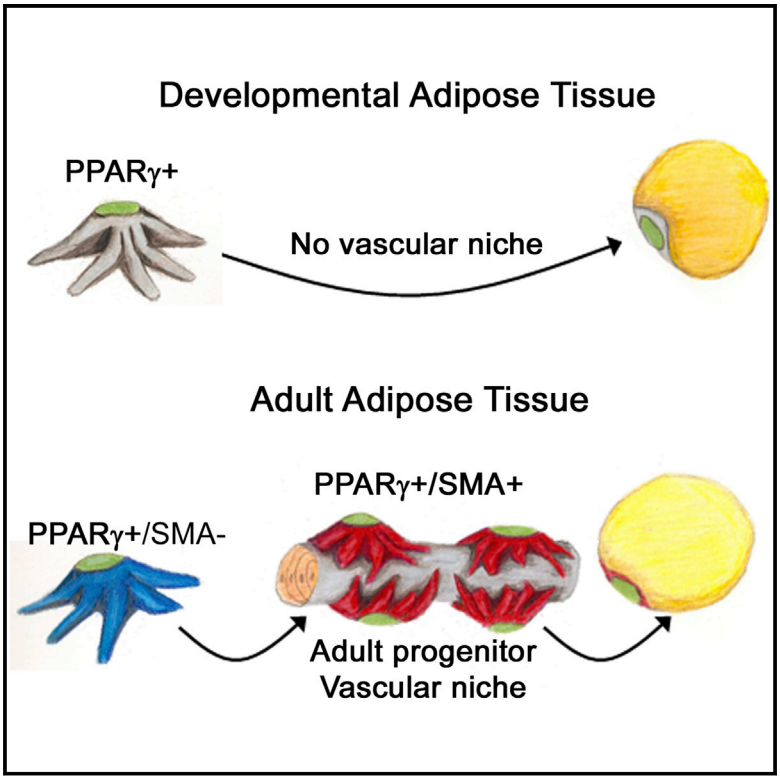

Authors

Yuwei Jiang, Daniel C. Berry, Wei Tang, Jonathan M. Graff

Correspondence

jon.graff@utsouthwestern.edu

In Brief

Adipose tissue development and progenitor cell specification are unclear. Jiang et al. identify two types of adipose progenitor cells, developmental and adult, that participate in organogenesis and homeostasis, respectively. Only adult progenitors fate-map from a smooth muscle actin mural lineage and are specified during embryogenesis, highlighting a potential therapeutic target for childhood and adult obesity.

Highlights

PPARγ+ progenitors are essential for adipose tissue organogenesis and homeostasis

Developmental and adult adipose progenitors show diverse features

Adult, but not developmental, adipocytes fate-map from a mural cell lineage

Adult progenitors are embryonically specified before developmental progenitors

Jiang et al., 2014, Cell Reports 9, 1007–1022
November 6, 2014 ©2014 The Authors
http://dx.doi.org/10.1016/j.celrep.2014.09.049

Cell Reports
Article

Independent Stem Cell Lineages Regulate Adipose Organogenesis and Adipose Homeostasis

Yuwei Jiang,[1,3] Daniel C. Berry,[1,3] Wei Tang,[1] and Jonathan M. Graff[1,2,*]
[1]Department of Developmental Biology
[2]Department of Molecular Biology
UT Southwestern Medical Center, Dallas, TX 75390-9133, USA
[3]Co-first author
*Correspondence: jon.graff@utsouthwestern.edu
http://dx.doi.org/10.1016/j.celrep.2014.09.049

SUMMARY

Adipose tissues have striking plasticity, highlighted by childhood and adult obesity. Using adipose lineage analyses, smooth muscle actin (SMA)-mural cell-fate mapping, and conditional PPARγ deletion to block adipocyte differentiation, we find two phases of adipocyte generation that emanate from two independent adipose progenitor compartments: developmental and adult. These two compartments are sequentially required for organ formation and maintenance. Although both developmental and adult progenitors are specified during the developmental period and express PPARγ, they have distinct microanatomical, functional, morphogenetic, and molecular profiles. Furthermore, the two compartments derive from different lineages; whereas adult adipose progenitors fate-map from an SMA+ mural lineage, developmental progenitors do not. Remarkably, the adult progenitor compartment appears to be specified earlier than the developmental cells and then enters the already developmentally formed adipose depots. Thus, two distinct cell compartments control adipose organ development and organ homeostasis, which may provide a discrete therapeutic target for childhood and adult obesity.

INTRODUCTION

Adipose depots develop in utero and during childhood (Birsoy et al., 2011; Tang et al., 2008). Once formed, white adipocytes store triglycerides and produce signals that regulate systemic metabolism (Rosen and Spiegelman, 2006; Spiegelman and Flier, 2001). During childhood and adult life, adipose depots protect against trauma and the cold and control a variety of processes such as thermoregulation and appetite (Rousseau et al., 2003). Adipose depots also appear to have adult-specific roles such as in fecundity, reproduction, and lifespan control (Hossain et al., 2007; Rosen and Spiegelman, 2006; Schwimmer and Haim, 2009; Spiegelman and Flier, 2001). Yet whether the stem cells that generate the two types of adipocytes, childhood and adult, are related is unknown (Prins and O'Rahilly, 1997). What appears clear is that forming and maintaining a relatively constant pool of adipocytes is essential for health; an excess (obesity) or deficit (lipodystrophy) of adipose tissue leads to metabolic dysfunction (Ailhaud et al., 1992; Gesta et al., 2007). Several lines of evidence, including human studies, indicate that new adipocyte formation is a key aspect of adult homeostatic balance and is required for maintenance and turnover throughout life (Faust et al., 1978; Johnson and Hirsch, 1972; Spalding et al., 2008). Further, obesogenic and other external stimuli appear to change the adipose turnover rate, and recent studies support the notion that such cues trigger formation of new adipocytes, possibly from an adipose stem compartment (Daniels, 2006; Hossain et al., 2007; Kopelman, 2000).

Tissue development and homeostasis often require a steady replenishment of cells from stem or progenitor sources (Weissman, 2000). These cells typically reside in a niche, a critical specialized microenvironment that regulates transitions of stem cells between quiescence, proliferation, and differentiation (Li and Clevers, 2010). Using a lineage marking system termed AdipoTrak (Tang et al., 2008), we recently began to identify and characterize a population of adipose progenitors that appear to have stem function and express PPARγ, a master regulator of adipocyte differentiation (Chawla et al., 1994; Tontonoz et al., 1994). For example, AdipoTrak-marked cells exhibit many canonical stem properties, such as their ability to self-renew, proliferate, and differentiate into adipocytes. In AdipoTrak, we recombined the tet-transactivator (tTA; "Dox Off" system) into the endogenous PPARγ locus (*PPARγ^{tTA}*) and combined this with complementary reporter systems (e.g., *TRE-H2B-GFP; TRE-Cre, R26R^{lacZ}*). Although the system has limited ability to mirror the dynamic expression of endogenous PPARγ, largely due to the long perdurance of *TRE-H2B-GFP* (Kanda et al., 1998) and the indelible marking of *R26R^{lacZ}*, AdipoTrak shows predominant adipose-restricted expression and can be effectively suppressed by doxycycline (Tang et al., 2008). Using these tools, we found that some AdipoTrak-marked cells resemble a subset of mural cells and localize to the perivascular region in established depots, which we postulated serves as an adipose progenitor cell niche (Tang et al., 2008). Mural cells, also termed pericytes or vascular smooth muscle cells denoting their expression of smooth muscle actin (SMA), reside at the vascular/periendothelial

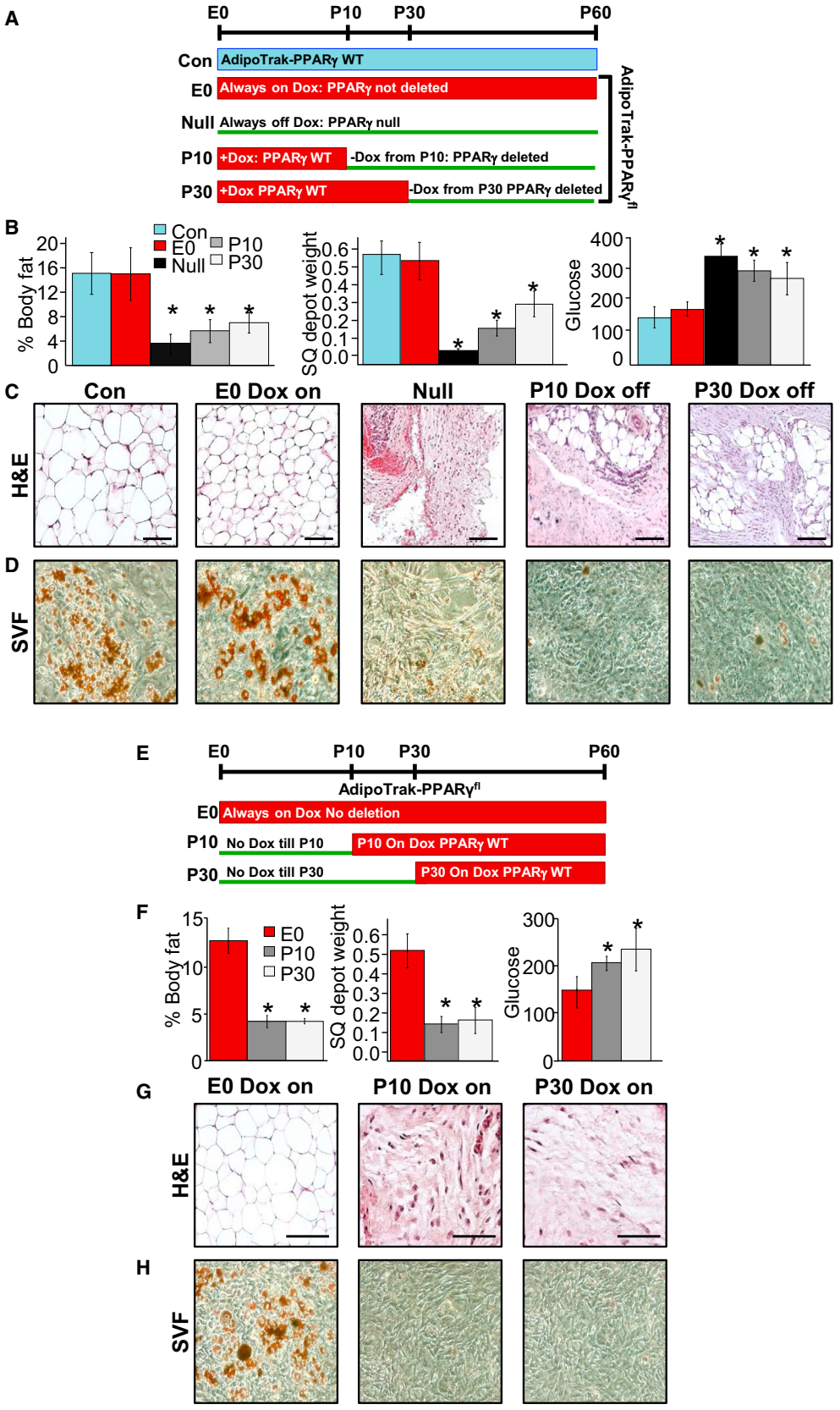

(legend on next page)

interface (Armulik et al., 2011). Yet no direct evidence exists that mural cells or AdipoTrak labeled cells are required for adipose tissue development or maintenance, and other localities such as the bone marrow and endothelium have been put forth as the origin of adipose stem cells (Cai et al., 2011; Crossno et al., 2006; Dani et al., 1997; Koh et al., 2007; Tran et al., 2012).

Here, we use the AdipoTrak system coupled with a mural cell-fate-mapping model (*SMA-Cre^{ERT2}*) and conditional PPARγ gene knockouts to investigate adipose lineage dynamics during both adipose development and adult tissue maintenance. We find that AdipoTrak-labeled cells appear to be key sources of adipose progenitors, and there appear to be two distinct AdipoTrak-marked adipose progenitor compartments, developmental and adult, that give rise to adipocytes during adipose tissue development and homeostasis, respectively. In established adult adipose depots, adipocytes fate-map from *SMA*+ progenitors residing in the perivascular niche, yet adipocytes from developing depots do not. Rather, developmental adipose progenitors are required for adipose depot formation and have distinct microanatomical, functional, and molecular properties compared to adult progenitors. Of note, the SMA+ adult progenitors are required for adult adipose tissue homeostasis and turnover; blocking their differentiation using a conditional PPARγ allele with either AdipoTrak or *SMA-Cre^{ERT2}* disrupts adipose depot structure and function. Interestingly, the adult progenitor lineage appears to be specified as early as embryonic day 10.5 (E10.5), significantly before the developmental progenitors, even though the role of the early-specified adult progenitors is later in life. In support of this notion, deleting PPARγ within these E10.5 AdipoTrak cells has no effect on adipose tissue development but does disrupt adult depot maintenance. Together, our data indicate that there are two distinct adipose progenitor compartments, developmental and adult, which are essential cellular components for adipose tissue formation and maintenance, respectively.

RESULTS

PPARγ-Expressing Progenitors Are Essential for Adipose Tissue Development and Homeostasis

Previous studies show that AdipoTrak (*PPARγ ^{tTA}; TRE-Cre; TRE-H2B-GFP)* cells fate-map into adipocytes during the development period and in adults (Tang et al., 2008). To examine the requirement of the AdipoTrak-labeled progenitor compartment during both depot formation and maintenance, we used the AdipoTrak system to constitutively or conditionally, in a temporally controlled manner, mutate PPARγ (*PPARγ$^{fl/tTA}$; TRE-Cre* = AdipoTrak-PPARγ$^{fl/tTA}$) (Ahmadian et al., 2013; Rosen et al., 1999; Tontonoz et al., 1994; Tontonoz and Spiegelman, 2008), thereby disrupting adipocyte differentiation in AdipoTrak progenitors (Figure S1A). These experiments are designed not to address the unequivocal requirement of the PPARγ gene in adipocyte formation but rather to test the potential necessity of AdipoTrak-labeled progenitors in fat formation and depot maintenance. We randomized, before conception, the parents of AdipoTrak-PPARγ$^{fl/tTA}$ mice to vehicle (AdipoTrak on, PPARγ null) or to doxycycline (Dox; which crosses the placenta and is incorporated into breast milk) suppressing PPARγ deletion, termed E0 for embryonic day 0, which we then continued in cohorts postweaning. AdipoTrak (*PPARγ$^{tTA/+}$; TRE-Cre)* served as controls. At P60, both the AdipoTrak control and AdipoTrak-PPARγ$^{fl/tTA}$ Dox-suppressed mice had normal adiposity, blood glucose, and tissue morphology (Figures 1B, 1C, and S1B), indicating that Dox suppression of PPARγ deletion was effective. However, PPARγ null mice displayed reduced adiposity, small adipose depots, hyperglycemia, disrupted tissue morphology, and reduced adipose tissue expression of PPARγ and downstream targets (Figures 1B, 1C, and S1B). This mutant resembles PPARγ null mice produced by epiblast deletion of PPARγ (Duan et al., 2007; Zeve et al., 2012). A potential caveat of this method is that PPARγ null disruption occurred in the AdipoTrak source before depot establishment, potentially disrupting depot formation or architecture, effects that might impede, mask, or preclude function of adipocyte progenitors in homeostatic responses. To circumvent this limitation and test the potential requirement of AdipoTrak-labeled progenitors in extant adipose tissue, we conditionally deleted PPARγ in already established depots with AdipoTrak-PPARγ$^{fl/tTA}$ at discrete times during depot development and homeostasis. In these studies, PPARγ deletion was Dox suppressed before conception and throughout embryogenesis. The Dox-suppressed mice were then randomized to continual Dox (E0) or Dox was removed at postpartum day 10 (P10; P10 Dox off) or P30 (P30 Dox off), to allow tTA activation, TRE-Cre expression, and PPARγ deletion (Figure 1A). At P60, both the P10 and the P30 Dox-off mutant mice displayed reduced adiposity, small adipose depots, hyperglycemia, disrupted tissue morphology, and reduced adipose tissue expression of PPARγ and downstream targets (Figures 1B, 1C, and S1B). At P60, we also evaluated the cell-autonomous adipogenic potential of stromal vascular (SV) cells, thought to contain adipose stem cells, isolated from control, E0 Dox-on, P10

Figure 1. AdipoTrak-Labeled Adipose Progenitors Are Required for Adipose Tissue Development and Homeostasis

(A) Experimental design. AdipoTrak-PPARγ$^{fl/tTA}$ mice were either maintained constitutively on Dox throughout life (suppressed, E0) or not on Dox throughout life (Null), or Dox was removed at the 10th or 30th day of life to induce deletion of PPARγ in AdipoTrak-labeled cells. AdipoTrak (*PPARγ$^{tTA/+}$; TRE-Cre*) mice were used as control.

(B) Body fat content, subcutaneous (SQ) depot weights, and random glucose levels of AdipoTrak (Con, no Dox), constitutively suppressed mutant (E0, Dox ON), constitutive deletion (PPARγ Null), P10 and P30 Dox off (PPARγ mutants); *$p < 0.05$ versus control levels.

(C) Hematoxylin and eosin (H&E) staining of adipose depots of mice described in (A).

(D) Oil red O staining of adipogencially induced SV cells isolated from the above mice at P60. Scale bar, 100 μm.

(E–G) Experimental design. AdipoTrak-PPARγ$^{fl/tTA}$ mice were administered Dox before conception or Dox was added at P10 or P30 (E) and at P60 mice were analyzed fat content, adipose depot weights, and glucose levels; *$p < 0.05$ versus control levels (F). (G) H&E-stained depots from mice described in (E).

(H) Oil red O staining of adipogencially induced SV cells isolated from mice in (E) at P60. Scale bar, 200 μm.

Data are expressed as mean ± SEM.

Dox-off, and P30 Dox-off mutant mice and cultured them in adipogenic media. The mutant cells did not display adipogenic potential based upon appearance, oil red O staining, triglyceride levels, and gene expression (Figures 1D, S1C, and S1D). Together, these data indicate that AdipoTrak-labeled progenitors are required for adipose tissue development and homeostasis.

Next, we attempted to address whether other potential non-AdipoTrak-labeled stem/progenitor cell sources, newly derived AdipoTrak or non-AdipoTrak adipocyte, arise after Dox suppression (stopping PPARγ deletion). For this approach, we added Dox at discrete times during adipose depot formation (P10 Dox on) or during adipose homeostasis (P30 Dox on) to suppress the tTA/TRE-Cre system and then block further deletion of PPARγ in potential new contributing adipose stem cells: either newly arisen AdipoTrak progenitors (derived from non-AdipoTrak sources) or possible other non-AdipoTrak sources. These potential cells should therefore contain a wild-type PPARγ, and if the cells have endogenous adipogenic potential, they should form or maintain normal depots or they should produce non-AdipoTrak-marked adipocytes, even when AdipoTrak progenitor differentiation has been impeded (Figure 1E). At P60, P10, and P30, Dox-on AdipoTrak-*PPARγ* mutant mice all showed similar lipodystrophic phenotypes: low body fat, a paucity of adipose tissue and adipocytes, hyperglycemia, and reduced expression of PPARγ and adipocyte markers (Figures 1F, 1G, and S1E), similar to the PPARγ-null phenotype in Figure 1C.

To examine stem cell-autonomous functions, we isolated SV cells from depots of these mutant mice and cultured the cells in Dox (to suppress tTA, thereby blocking any in vitro PPARγ deletion in any new potential sources) and adipogenic conditions. Under these conditions, the SV cells did not differentiate, indicated by the lack of the oil red O staining, reduced triglyceride levels, and gene expression (Figures 1H, S1F, and S1G). Together, the data suggest that AdipoTrak-labeled progenitors are required and appear to be a major source for adipose tissue development and possibly homeostasis.

Adult Adipocytes Derive from an SMA+ Mural Cell Source

We previously observed that AdipoTrak-GFP-marked cells resemble mural cells residing in the perivascular region of mature adipose depots (Tang et al., 2008). This appearance and several other indirect studies indicated that the vessel might serve as an adipose progenitor niche (Cai et al., 2011; Gupta et al., 2012; Han et al., 2011). Niche residence is a central feature of adult stem cells and is often acquired toward the end of the developmental phase, which for murine depots is in the first few postpartum weeks. Consistent with that notion, we found that at earlier stages of adipose organogenesis (P10), progenitors reside off the blood vessel, but at P30, in already formed depots, marked cells have occupied mural perivascular positions (Figure 2A). By P20, the cells appeared juxtaposed to the vessel, but primarily in nonmural positions with a subset in the vessel wall per se (Figure 2A). Stromal vascular particulates (SVP), an organotypic method to study the niche within its native context (Tang et al., 2008), also show the same adipose progenitor localization: none in the blood vessels at P10, many at mural positions at P30, and P20 in transition (Figure 2B). Thus, it appears that during adipose tissue development, AdipoTrak-marked cells reside off the vessel, whereas within mature established adipose tissue, they reside on the blood vessel.

To determine whether mural cells contribute to adipose tissue development and/or adipose tissue homeostasis and turnover, we combined AdipoTrak-GFP marking with a tamoxifen (TM)-inducible *SMA-Cre^{ERT2}* fate-mapping model using two independent indelible Cre reporter lines: *R26R^{lacZ}* and *R26R^{RFP}* (Figure S2A). This system is designed for long-perdurance GFP adipose lineage marking (*PPARγ^{tTA}; TRE-H2B-GFP*) (Kanda et al., 1998; Tang et al., 2008), while the Cre-dependent reporters are intended to label the mural cell lineage and all descendants, in an indelible fashion (*SMA-Cre^{ERT2}*; *R26R^{lacZ}* = *SMA-lacZ* or *SMA-Cre^{ERT2}*; *R26R^{RFP}* = *SMA-RFP*) (Wendling et al., 2009). The *SMA-Cre^{ERT2}* fate-mapping model was generated from a bacterial artificial chromosome construct reported to have high-fidelity expression (Wendling et al., 2009). We induced SMA-dependent recombination by providing one dose of TM on two consecutive days at P10 (organogenesis) or P30 (established depots for adipocyte turnover and maintenance) and examined reporter expression either on the third day (P12 or P32, pulse) or at P60 (pulse-chase) (Figures 2C, 2D, S2B, and S2C); siblings that did not receive TM served as controls (Figure S2D). At the short time frames (P12 or P32, pulse), SMA-dependent reporter expression (e.g., red fluorescent protein [RFP], lacZ) was restricted to perivascular mural cells, as reported previously (Armulik et al., 2011; Nehls and Drenckhahn, 1993; Wendling et al., 2009), and mature adipocytes were not labeled (Figures 2D, S2B, and S2C). During the P10 to P60 pulse-chase, we again observed strong perivascular, without adipocyte, labeling in subcutaneous (SQ; inguinal, interscapular) and visceral (Vis, perigonadal, retroperitoneal) depots with either RFP or LacZ (Figure 2E, top row, and Figure S2E). Yet during the P30 to P60 pulse-chase, reporter expression evolved with labeling of both SQ and Vis depots with either RFP (Figure 2E, bottom row, and Figure S2E) or lacZ indelible reporters (Figure S2C). The different fate-mapping observations did not appear to stem from the elongated pulse-chase protocol of the P10 mice (P10–P60 versus P30–P60), as a P30–P90 chase labeled adipose depots (Figure S2F). These data support the notion that P30 SMA+ cells give rise to adipocytes.

During the developmental phase (organogenesis), adipose depots undergo rapid expansion and potentially increase turnover (Rigamonti et al., 2011; Spalding et al., 2008; Tang et al., 2008). To examine the possibility that rapid adipose tissue turnover during this time frame might obscure SMA fate mapping, we performed a shorter chase (P10–P30), but again SMA+ cells did not contribute to adipocyte formation (Figure S2G). A P3 to P30 pulse-chase also generated perivascular labeling, but not adipocyte fate mapping (data not shown). To examine if these early *SMA-Cre^{ERT2}*-marked cells were utilized later in the adult, we fate mapped from P10 to P180, but again only the perivascular region appeared labeled (Figure S2H). However, a P90 to P120 *SMA-Cre^{ERT2}* chase produced strong depot labeling (Figure S2I), indicating that SMA+ cells are used as a source of

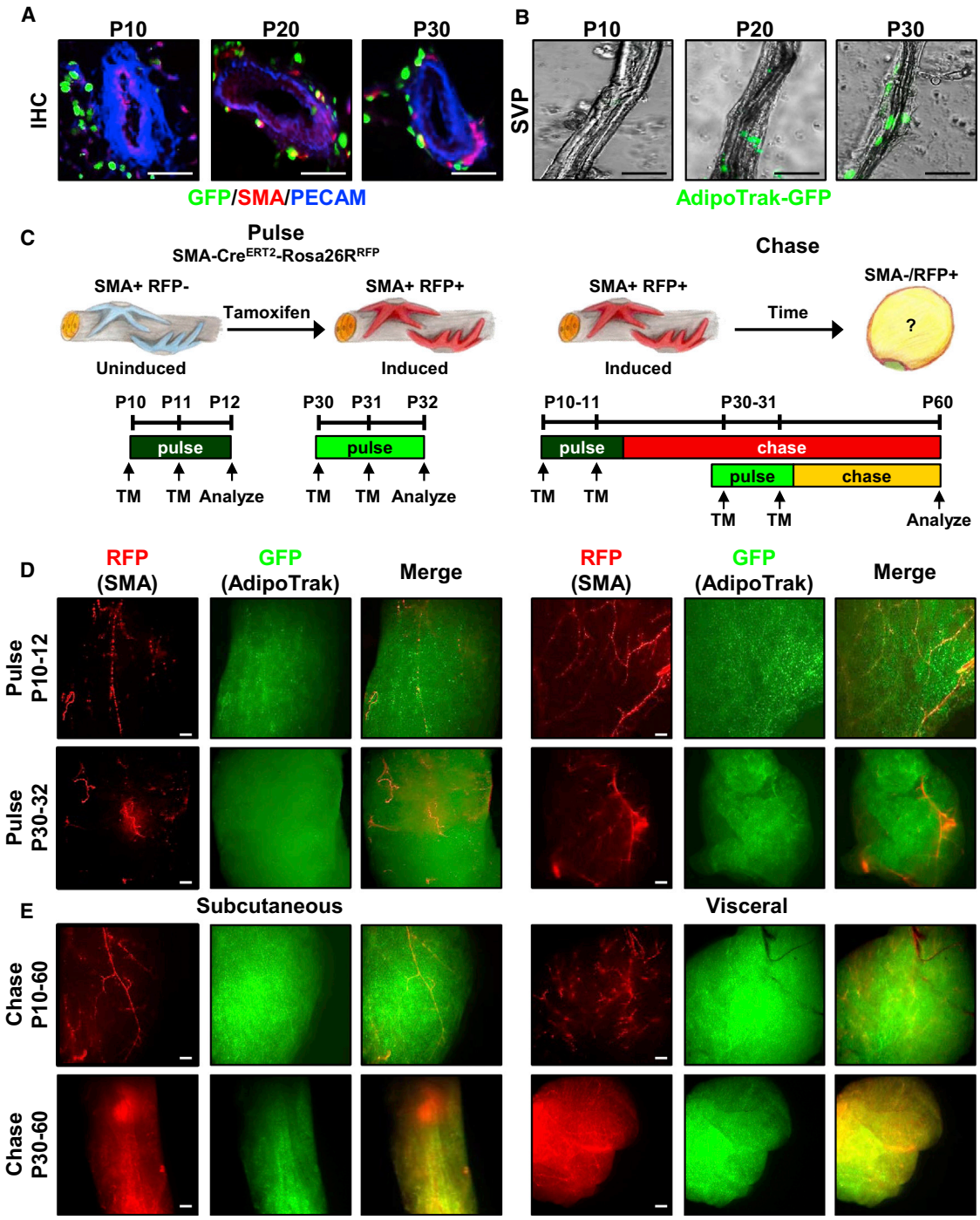

Figure 2. Adult Adipocytes Derive from a Mural Cell Source

(A) Sections from P10, P20 and P30 AdipoTrak-GFP SQ depots were examined for GFP (green), PECAM (blue), and SMA (red). Scale bar, 100 μm.

(B) GFP fluorescent images of SVPs isolated from P10, P20, and P30 AdipoTrak SQ depots.

(C) Cartoons and schema depicting fate-mapping analysis. *SMA-Cre* ^{ERT2}*; R26R*^{RFP} are induced with TM for 2 consecutive days at either P10 or P30 and then analyzed at P12 or P32 or chased to P60.

(D and E) AdipoTrak-GFP (*PPARγ*^{tTA}*; TRE-H2B-GFP*); *SMA-Cre* ^{ERT2}*; R26R*^{RFP} mice were administered TM at P10 or P30 for 2 consecutive days, and SQ (inguinal) and Vis (perigonadal) adipose depots were examined for GFP (adipose lineage) and RFP (mural lineage) fluorescence either at pulse (P10–P12 or P30–P32) (D) or chase (P10–P60 or P30–P60) (E). See Figure S2A for experimental genotypes. Scale bar, 100 μm.

progenitors for adipocytes throughout the adult depot life cycle, but not during depot organogenesis.

Developmental and Adult Adipose Progenitors

To dissect the cellular basis of the lineage specification, we next examined adipose tissue sections from AdipoTrak-GFP; SMA-RFP mice (GFP marks adipose lineage, RFP marks mural lineage and descendants) pulsed with TM at P10 or P30 and chased to P60. The P30 initiated pulse-chase specimens displayed RFP+ unilocular adipocytes that immunostained with Perilipin, an adipocyte marker, and costained with LipidTox, but the P10 samples did not (Figures 3A and 3B). Quantification indicated that about 25% of all adipocytes were labeled by the *SMA-Cre^{ERT2}* system between P30 and P60, a proportion that aligns with previous studies of percentages of adipocytes labeled over this period (data not shown) (Tang et al., 2011). During this 30-day chase, we also visualized RFP signal in floating P30–P60 pulse-chase adipocytes, isolated by density centrifugation, but not in P10–P60 adipocytes (Figure 3C). We next examined the in vitro adipogenic potential of P10 and P30 TM-pulsed *SMA-RFP* SV cells, containing both SMA+ and SMA− cells. Although the SV fraction from either P12 or P32 appeared equally adipogenic, based upon oil red O staining, gene expression and triglyceride quantification (Figures 3D, S3A, and S3B), only P32 SV cells produced RFP+ adipocytes (Figure 3E), indicating that they derived from an SMA lineage. Further, the brief TM pulse labeled >75% of the SV-formed adipocytes (not shown). Together, these data indicate that at least a subset of mural cells function as adipose progenitors for depot maintenance and also support the possibility that adipose organogenesis derives from a distinct source.

We next assessed the specificity of *SMA-Cre^{ERT2}* labeling, especially at P30, when the marked cells have acquired adipose progenitor function. As a step, we examined histological specimens of P12 or P32 AdipoTrak; *SMA-RFP* depots after either a P10 or P30 TM pulse, respectively. We found that robust RFP expression aligned in mural positions on depot vasculature that coimmunostained with multiple mural markers such as SMA, NG2, and PDGF-Rβ, but not with endothelial markers (e.g., PECAM) (Figures 3F and S3D–S3F), as reported previously (Armulik et al., 2011). Consistent with this, flow cytometric studies showed that the vast majority of RFP+ cells costained with SMA, indicating high correspondence to endogenous expression (Figures 3G and S3C). Other well-established mural markers were also expressed on the majority of RFP+ cells; approximately 75% of the RFP+ cells expressed NG2 and PDGF-Rβ (Figure 3G). Cell-surface phenotyping also showed coexpression of several proposed adipose stem cell markers: the majority of the RFP-marked cells expressed Sca1 and CD24, and about half expressed CD34 and PDGF-Rα (Figure 3G). Furthermore, quantitative PCR analyses of flow-sorted SMA-driven RFP+ SV cells compared to flow-sorted RFP− cells showed that SMA-traced cells had significant enrichment of *PPARγ* and *Zfp423*, an adipose progenitor marker (Gupta et al., 2010), and a battery of mural cell markers; RFP− cells were enriched in endothelial marker expression (Figure 3H). In agreement with previous reports, SMA-dependent reporters also marked mural cells of vessels in other organs (Figures S3G–S3I) (Wendling et al., 2009). Together, these data indicate that the *SMA-Cre ^{ERT2}* marking system has high fidelity and the expected specificity: SMA-dependent reporters are expressed in mural microanatomic positions, and their genetic signature resonates with mural profiles.

Morphogenetic Properties of Developmental and Adult Adipose Progenitors

To examine the possibility of two adipose progenitor sources/compartments, we employed our AdipoTrak-GFP; *SMA-RFP* mice, which allow independent, and comparative, analyses of the adipose lineage (GFP+) and the mural lineage (RFP+). Flow cytometric quantification indicated that many P30 AdipoTrak-GFP-positive SV cells colabeled with RFP, but P10 GFP+ cells did not (Figure S4A). Similarly, P30 *SMA-RFP*-positive SV cells colabeled with GFP, but P10 RFP+ cells did not (Figure S4B). Analyses of TM-pulsed P10–P12 and P30–P32 adipose sections indicated that P10 GFP+ adipose progenitors did not reside at the vascular interface, whereas P30 GFP+ adipose progenitors did (Figure 4A). SVPs also showed the same adipose progenitor cell pattern: GFP marked stem cells that costained with RFP present in blood vessels at P30, but not at P10 (Figure 4B). These distinguishable features (e.g., microanatomic and fate-mapping) prompted us to refer to "developmental" adipose progenitors and "adult" adipose progenitors, as they might be different cell types.

To test whether the difference in niche localization of the developmental and adult adipose progenitors might be due to inherent morphogenetic properties, we assessed several explant, in vitro, and molecular correlates. To explore vasculogenic and nichegenic potential, we explanted portions of P10, P20, and P30 AdipoTrak-GFP depots, encased them in Matrigel, and monitored the explants for vascular outgrowths (Gealekman et al., 2008; Han et al., 2011). All explants produced capillary outgrowths; however, the P30 depots had longer and denser vascular sprouts and higher GFP+ progenitor cell occupancy, whereas the P20 depots had an intermediate phenotype (Figures 4C, 4F, and 4G). Next, we examined the migratory potential of fluorescence-activated cell sorting (FACS)-isolated GFP+ developmental and adult adipose progenitors in a scratch-motility assay. We found that P20 and P30 progenitors had higher migratory rates than P10 progenitors; P30 cells had the highest motility (Figures 4D and H). We also utilized transwell plate and modified Boyden chamber assays (Chen, 2005), first monitoring the ability of FACS-isolated GFP+ adipose progenitors to move from one chamber to another. We again observed the same trend: P10 cells with the lowest migration, P20 cells in the middle, and P30 progenitors showing the greatest potential (Figures 4E and 4I). We next probed the possibility that SV cells, containing endothelial and other cells that constitute the niche, might alter adipose progenitor movement. For this, we placed FACS-isolated P10 and P30 GFP+ progenitors in one chamber and age-matched SV cells in the other. We also performed reciprocal migration assays with age-mismatched SV cells: P10 adipose progenitors with P30 SV cells, and P30 progenitors with P10 SV compartment. We found that P10 progenitors had an overall lower migratory potential that appeared unaffected by either SV compartment (Figure 4J).

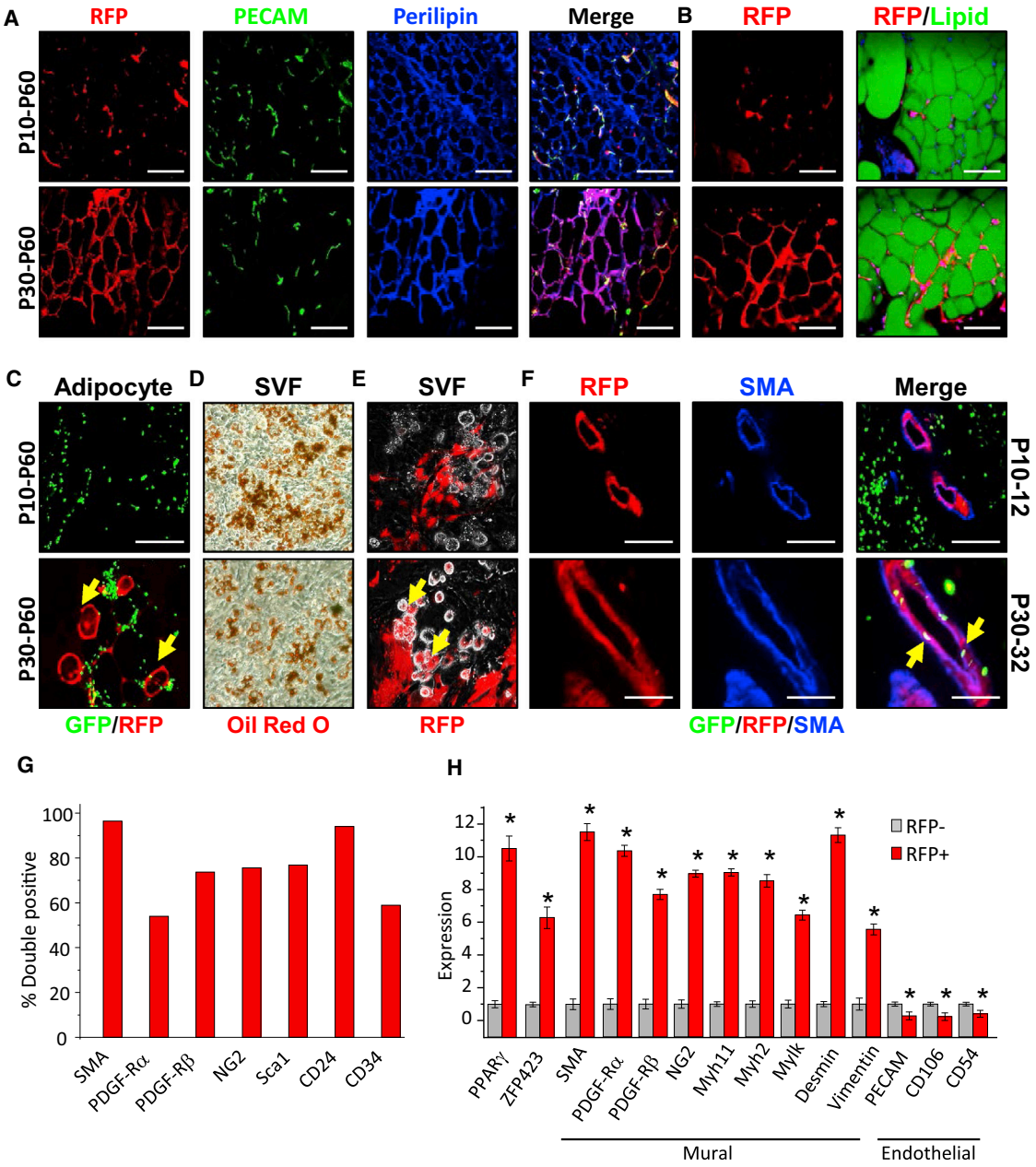

Figure 3. Developmental and Adult Adipose Progenitors Have Distinct Lineages and Localities

(A–C) AdipoTrak-GFP; SMA-RFP mice were administered TM at P10 or P30 and chased to P60. (A) Sectioned SQ depots were analyzed for RFP and immunostained for PECAM (green) and Perilipin (blue) or (B) RFP and LipidTox (lipid) staining. (C) Floated adipocytes were examined for RFP (mural lineage) and GFP (adipose lineage). Yellow arrows indicate colocalization between AdipoTrak-GFP- and SMA-RFP-labeled adipocytes.

(D and E) One day after a P10 or P30 TM pulse, AdipoTrak-GFP; SMA-RFP SV cells were isolated, cultured in adipogenic conditions, and oil red O (adipocyte) stained (D) or examined for RFP fluorescence (E). Yellow arrows (E) indicate SMA-RFP-labeled adipocytes.

(F) Two days after a P10 or P30 TM pulse, AdipoTrak-GFP; SMA-RFP depots were examined for RFP and GFP expression and immunostained for SMA. Yellow arrows indicate AdipoTrak-GFP; SMA-RFP-labeled progenitors in a perivascular position at P30.

(G and H) FACS analyses (G) and mRNA analyses (H) of denoted genes in FACS-isolated RFP+ or RFP− cells from SMA-RFP mice 2 days post TM injection. *$p < 0.01$ RFP+ versus RFP− cells. Scale bar, 100 μm.

Data are expressed as mean ± SEM.

Notably, the potential of the P30 progenitors to migrate was stimulated by age-matched SV cells, whereas the P10 SV cells inhibited P30 progenitor migration (Figure 4J). Molecular analyses supported the functional tests: FACS-isolated adult adipose progenitors (P30) had significantly higher levels of mural cell (e.g., *SMA*, *PDGF-Rß*, and *NG2*) and vasculogenic (e.g.,

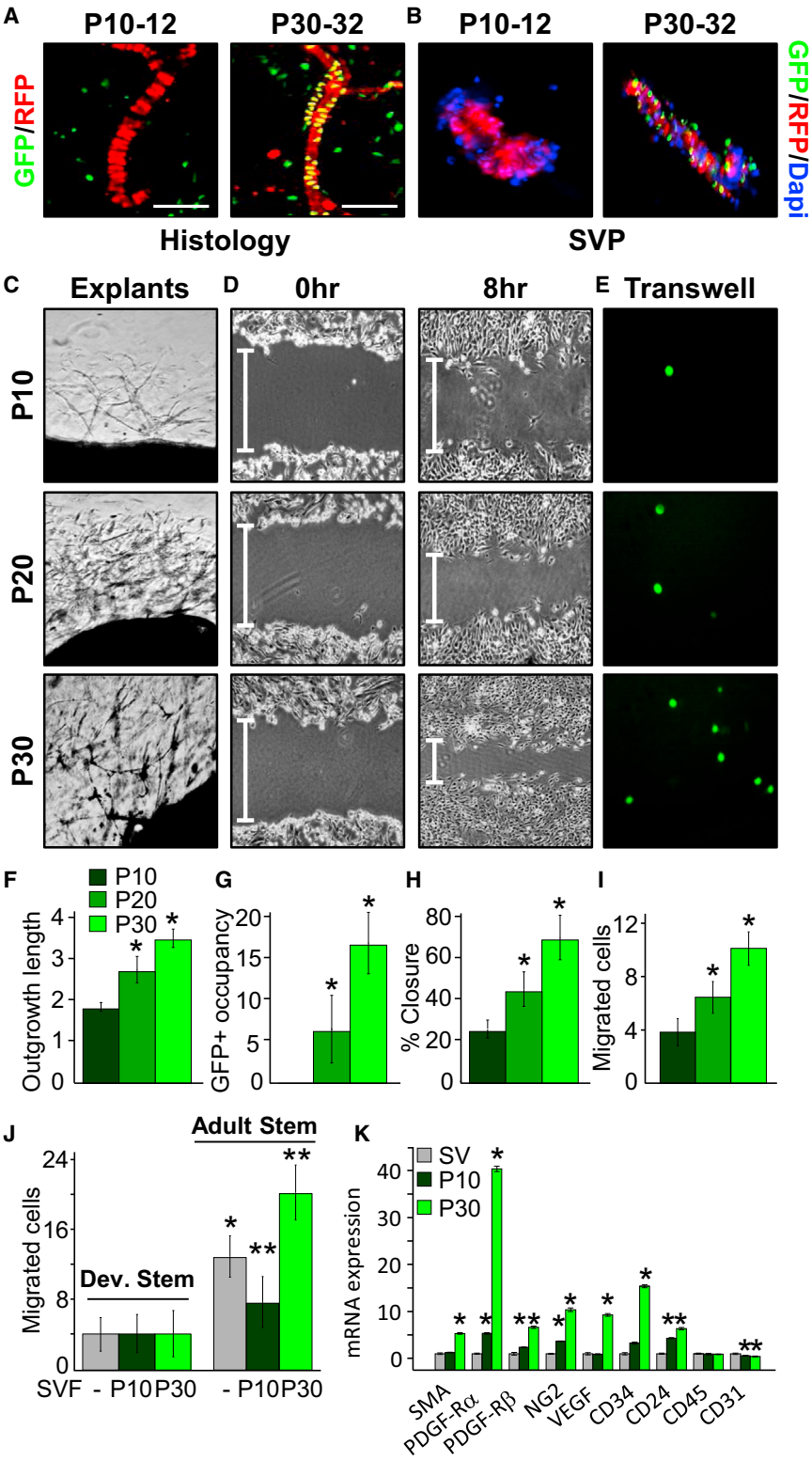

Figure 4. Functional and Molecular Characteristics of Developmental and Adult Adipose Progenitors

(A and B) RFP and GFP images of sectioned SQ depots from TM pulsed (P10–P12, P30–P32) AdipoTrak-GFP; SMA-RFP mice. Scale bar, 200 μm.

(B) SVPs were isolated from the above mice (A) and examined for RFP and GFP expression and counter stained with DAPI (nuclear, blue).

(C, F, and G) P10, P20, and P30 AdipoTrak SQ depots were encased in Matrigel, and 7 days later, capillary outgrowth was assessed with pseudo-Nomarski microscopy (C), length quantification (F), and GFP+ stem cell occupancy (G).

(D and H) P10, P20 or P30 AdipoTrak FACS-isolated GFP SV cells were cultured to confluence and scratched, and migration was visualized (D) and quantified (H).

(E and I) P10, P20, or P30 AdipoTrak FACS-isolated GFP+ SV cells were placed in a modified Boyden chamber. Transwell migration was imaged 12 hr later (C) and quantified (G).

(J) P10 and P30 FACS-isolated GFP+ cells were placed in one chamber and no cells (–), P10, or P30 SV cells in the other. GFP cell transwell migration was quantified 12 hr later. **$p < 0.05$ versus P30 stem cell migration without SV cells.

(K) Quantitative PCR expression analyses of P10 or P30 FACS-isolated GFP+ SV cells.

For (F)–(K), *$p < 0.05$ versus P10 stem cells.

VEGF-A) markers, which were low or undetectable in isolated developmental adipose progenitors (P10) (Figure 4K). Flow cytometric studies also showed an enrichment of mural markers in P30 AdipoTrak-marked progenitors, with the majority of GFP+ cells coexpressing mural markers, and that coexpression of a variety of proposed adipose progenitor markers such as CD34, SCA1, CD24, and PDGF-Rα were similar in developmental and adult progenitor populations (Figures 4K and S4B). Taken together, the data indicate that adult adipose progenitors have distinct functional properties and molecular profiles compared to developmental adipose progenitors, and that might account for their different niche localities.

Mural Resident Progenitors Contribute to Adipose Depot Homeostasis

The AdipoTrak PPARγ deletion studies indicated a required role of the AdipoTrak-marked progenitors in both adipose depot organogenesis and homeostasis (Figure 1). However, the distorted depot architecture that results from early or late loss of PPARγ might preclude stem function of potential new stem cells in the Dox-on studies, possibly even in the isolated stromal vascular fraction (SVF) setting. Further, expression of AdipoTrak throughout the adipose lineage (stem cells to

adipocytes) or in other cell types may confound the Dox-off analyses. For example, AdipoTrak-induced deletion of PPARγ in extant adipocytes might change the character of the depot even in the absence of changes in stem cell function. To probe the specific contribution of mural-resident adult adipose progenitors, we conditionally deleted PPARγ with the *SMA-Cre*^{ERT2} mural cell driver (*SMA-Cre*^{ERT2}, *PPARγ*$^{fl/fl}$ = *SMA-PPARγ*) that appears to be specific to the progenitors and is not expressed in adipocytes per se at pulse but does fate-map into adipocytes thereafter. We induced PPARγ deletion by administering one dose of TM on two consecutive days starting at P30, a time when SMA+ AdipoTrak+ cells are present in the mural perivascular niche. As a control, we also induced SMA-dependent deletion at P10 when SMA-negative, nonmural resident AdipoTrak+ developmental adipose progenitors are present. We analyzed the adipose phenotypes 4 weeks later (Figures 5A and S5A). Consistent with the SMA fate-mapping studies (Figures 2 and 3), we observed no significant adipose phenotypes when PPARγ was deleted within the SMA lineage at P10; body fat content, adipose tissue size, histology, fed glucose, sera triglycerides, adipose gene expression, and glucose tolerance were similar to controls (Figures 5B, 5D, 5E, S5B, S5C, and S5F). In contrast, deletion of PPARγ in P30 SMA+ cells resulted in reduced fat content (similar to their initial fat content), smaller depots with aberrant histology, hypertriglyceridemia, and altered adipose molecular profile and glucose intolerance (Figures 5C–5E and S5D–S5F). To track progenitor autonomous functions, we also *SMA-Cre*^{ERT2} fate mapped in the setting of PPARγ disruption. Notably, P30 PPARγ-null SMA+ cells did not give rise to RFP+ adipocytes, resembling the lack of *SMA-RFP* adipocyte fate mapping of P10 mice, whereas control P30 SMA+ cells expressing PPARγ did (Figure 5G).

The fate-mapping data supported a progenitor-specific defect, but PPARγ may also have roles in SMA vascular cell function that could affect depot integrity. To assess this possibility, we quantified whole depot expression of several vascular markers (e.g., *SMA*, *NG2*, *PDGF-Rα*, and *PECAM*) in either deletion setting, yet the levels appeared unchanged (Figure 5E). We also histologically examined other organ systems and found no histological differences when *SMA-PPARγ* deletion was induced at either P10 or P30 (Figures 5F and S5G). Further, there was no evidence of vascular changes or vascular leakage in these organs or in depots (Figures 5F and S5G, data not shown). Thus, deleting PPARγ in P10 and P30 SMA+ cells produce similar vascular phenotypes between P10 and P30 chases, indicating that vascular dysfunction is unlikely to be the primary instigator of adipose tissue effects.

To further evaluate potential cell autonomy (that is, progenitor-specific effects), we repeated the P10 and P30 TM pulses, collected SVF at P12 and P32, and cultured the cells in adipogenic conditions. The adipogenic potential of P10-pulsed SV cells appeared normal; in contrast, the P30 mutant SVF failed to differentiate indicated by the lack of the oil red O staining and reduced adipocyte marker expression (Figures 5H and S5H). We also examined potential cell autonomy by isolating P30 SV cells from uninduced *SMA-PPARγ* mice, ie, from depots that are unaffected and have normal vasculature and depot integrity. We then cultured the cells in adipogenic media containing either vehicle or TM. Within 48 hr of TM addition to induce *SMA-PPARγ* deletion in cell culture, *PPARγ* expression was reduced, yet levels of vascular markers (*SMA*, *NG2*, *PDGF-Rα*, and *PECAM*) were unchanged (Figure S5I). Consistent with the reduction in PPARγ expression, SV cells from *SMA-PPARγ* mice that received TM did not undergo adipocyte differentiation, whereas vehicle-treated cells underwent adipogenesis as indicated by adipocyte marker expression (Figure S5J). Together, the *SMA-PPARγ* genetic models provide in vivo and in vitro functional and molecular support for the notion that mural cells act as adipose progenitors, but only in established adult depots and not during adipose development.

Adult Adipose Progenitors Are Specified Earlier than Developmental Progenitors

Next, we attempted to unravel the lineage relationship between the developmental and adult progenitors, exploring whether developmental progenitors might evolve into adult progenitors or whether the two progenitor compartments might have independent origin. To delineate the temporal pattern of adipose lineage specification, we combined AdipoTrak with R26R^{lacZ} (AdipoTrak-lacZ = *PPARγ*$^{+/tTA}$*; TRE-Cre; R26R*^{lacZ}) to indelibly label adipose progenitors. We treated cohorts of AdipoTrak-lacZ mice with placebo or Dox to suppress tTA activity, thereby blocking any new lacZ expression. We added Dox at regular intervals during embryogenesis and in the peripartum period when adipose organogenesis occurs. We then analyzed all offspring for lacZ expression at P30, when depots are already established and the adult progenitors have occupied niche positions (Figures 2 and 3). In this situation, adipose progenitors will be indelibly labeled by β-galactosidase only if the stem compartment was specified prior to Dox addition, evolved, and underwent adipogenesis. This can be visualized in whole-mount stains: adipocytes and depots become blue (Xgal+). We found that specification occurred in a defined sequence: SQ adipose developmental progenitor (inguinal and interscapular) marking began about E14.5 and was completed by P2, retroperitoneal developmental progenitor marking started by E18.5 and was completed by P4, perigondal developmental progenitor marking began as early as P4 and continued until P10, and mesenteric adipose depot developmental progenitor marking was apparent at P15 and continued until P20 (Figure 6A).

To determine when the adult progenitor cell compartment was specified, we examined histological sections of the just-described depots for the presence of lacZ+ cells within the vasculature. First, we analyzed the vessels of depots in which the developmental lineage had been specified as indicated by blue adipocytes in the whole-mount setting (e.g., inguinal with Dox added from E14.5 on, PGW after P6 Dox, etc.). All harbored AdipoTrak-lacZ lineage-positive cells in the vessel, indicating that both developmental and adult progenitor compartments had been specified (Figure S6A, bottom). Remarkably, even when we examined depots that were whole-mount lacZ negative (i.e., Dox was added before developmental progenitor specification/marking), we observed AdipoTrak-lacZ-positive cells lining the blood vessels. For example, E16.5 +Dox retroperitoneal

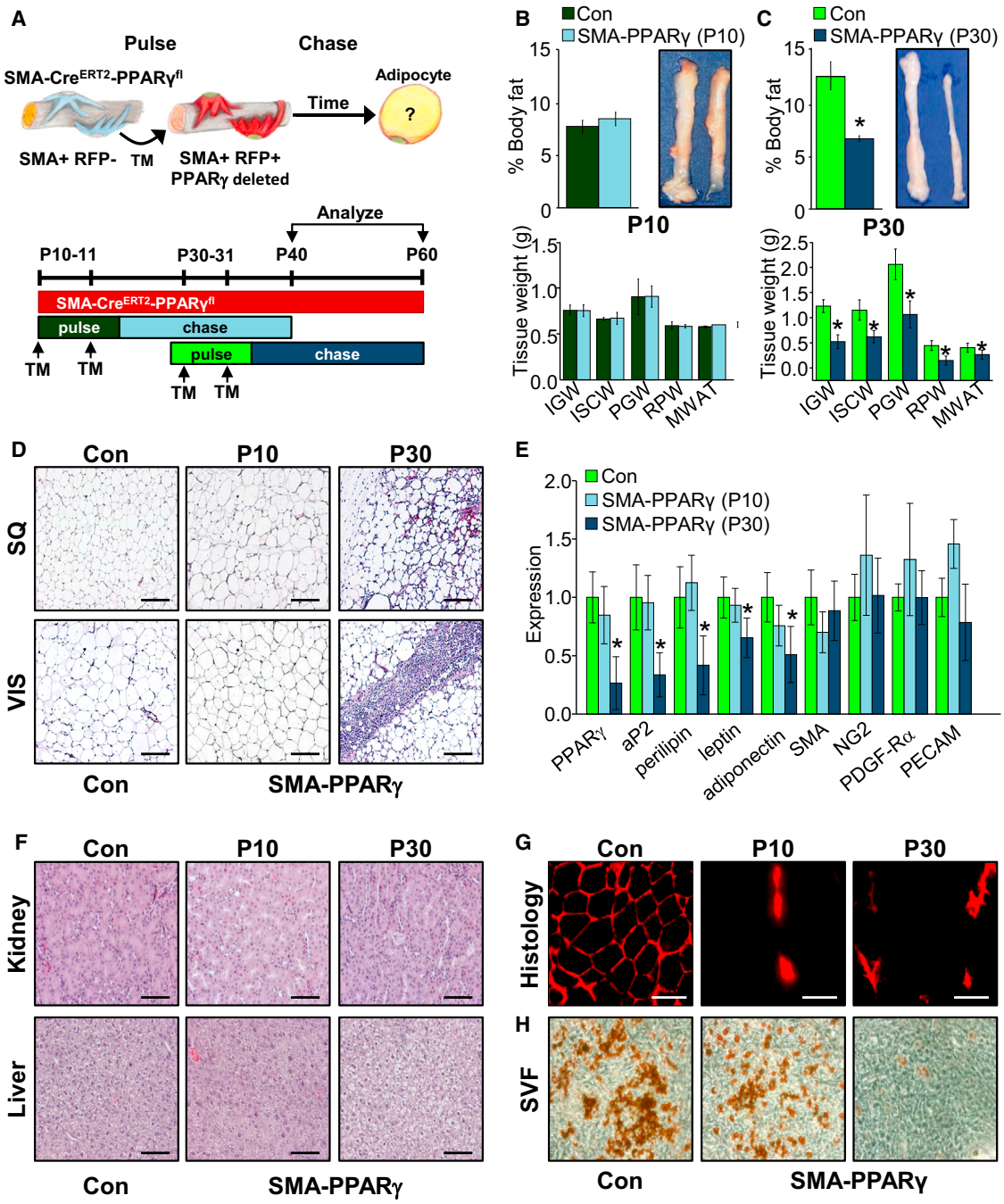

Figure 5. Mural Cells Contribute to Adult Adipose Tissue Homeostasis

(A) Experimental design. Top: cartoon depicting the experimental test, where PPARγ is temporally deleted in SMA+ cells during developmental or adult adipose stages. Bottom: experimental protocol used to test if SMA mural cells are required for adipose tissue homeostasis. *SMA-PPARγ* mice (*SMA-Cre*^{ERT2}, *PPARγ*$^{fl/fl}$) were administered TM at P10 or at P30.

(B–G) Four weeks later (P40 or P60), they were analyzed: fat content and depot size (B and C), depot weights (B and C), H&E staining of SQ and Vis adipose tissues (D), whole-depot marker expression (E), H&E staining of kidney and liver (F), and RFP fate mapping (G). *$p < 0.05$ versus controls.

(H) SV cells were isolated 2 days after TM injection and cultured in adipogenic media, and adipogenic potential was assessed by oil red O staining.

Data are expressed as mean ± SEM.

white adipose tissue depots show perivascular mural lacZ marking without adipocyte staining, and these mural resident lacZ+ cells were PECAM negative (Figure S6A, top). These data support the unexpected possibility that the adult adipose progenitor compartment is specified prior to the developmental compartment.

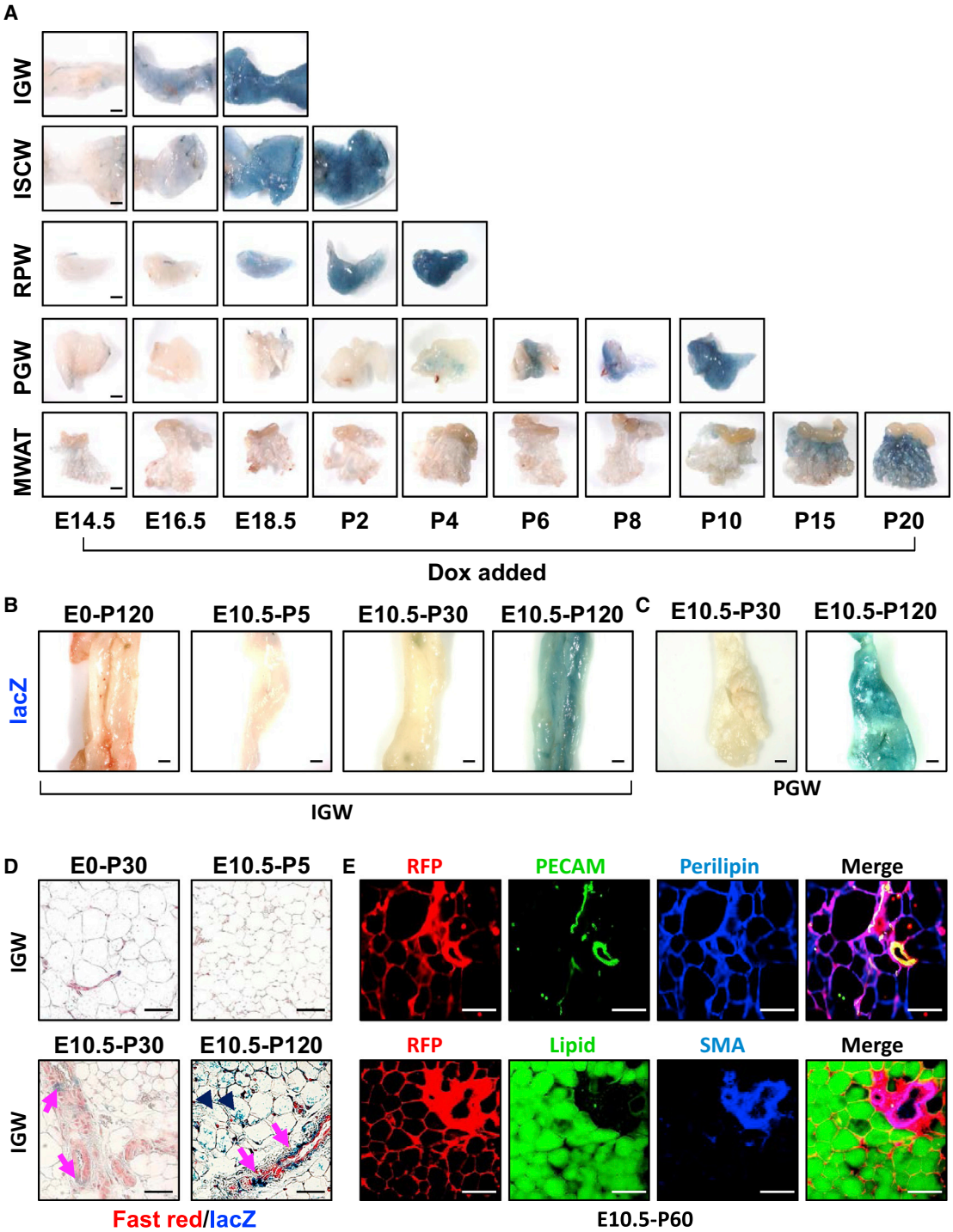

Figure 6. Temporal Course of AdipoTrak Labeling of Adipose Progenitors

(A) AdipoTrak, R26R^{lacZ} mice were Dox suppressed at the denoted times, and each adipose depot was analyzed at P30 for β-galactosidase activity.

(B and C) AdipoTrak, R26R^{lacZ} mice were Dox suppressed at the indicated times (E0 = preconception, or E10.5) and SQ depots (B) examined at P5, P30, or P120 or perigonal adipose depot (C) examined at P30 or P120 for β-galactosidase activity.

(D) AdipoTrak, R26R^{lacZ} mice were Dox suppressed from E0 to P30 (control) or from E10.5 to P5, P30, and P120, and adipose depots were stained with X-gal, sectioned, and stained with nuclear fast red. Arrows indicate AdipoTrak cells that were marked by E10.5 and present in adult adipose depot vessels; arrowheads indicate X-gal-labeled adipocytes that derived from cells marked by E10.5.

(E) Immunofluorescence images of adipose depot sections of AdipoTrak R26R^{RFP} mice that were Dox suppressed from E10.5 to P60 and visualized for RFP (AdipoTrak lineage) and costained with either PECAM or LipidTox (green) and Perilipin or SMA (blue). Scale bar, 200 μm.

To begin to probe when the adult compartment was first marked by AdipoTrak, we examined a series of postimplantation embryos for GFP expression using AdipoTrak-GFP mice. Prior to E9.5, we did not detect GFP expression (data not shown). Yet by E10.5, a small number of GFP+ cells were present in the anterior region of the embryo in the vicinity of developing nervous system, neural crest, and notochord (Figure S6B). This pattern appeared to expand and elaborate, with cells appearing in a rostral to caudal migratory stream over the ensuing embryonic days (Figures S6B–S6E).

To assess whether some of these embryonically marked cells might fate-map into vascular-resident adult adipose progenitors, we returned to the AdipoTrak-R26R^{lacZ} indelible-labeling model. We also ingressed the *R26R^{RFP}* reporter, described above in the SMA tracking system, and generated AdipoTrak-RFP (*PPARγ$^{+/tTA}$; TRE-Cre; R26R^{RFP}*) cohorts in part to ease scoring with direct fluorescence. We provided AdipoTrak-lacZ and AdipoTrak-RFP cohorts with either vehicle or Dox, to block any further de novo marking, at E10.5, the developmental stage in which we observed anterior GFP staining and before any developmental progenitors are specified. We then assessed potential adipose-depot fate mapping at P5, P30, P60, and P120 (Figure S6F). We observed E10.5 adipocyte fate mapping for both reporters, R26R^{RFP} and R26R^{lacZ}, by P60, but not at P5 or P30 (Figures 6B–6E, S6G, and S6H). However, we did observed E10.5 AdipoTrak fate mapping onto vessels at P30, but not at P5 (Figures 6D, S6G, and S6H), consistent with the data set examining whole mounts for developmental specification (Figures 6B and 6C). That is, P30, but not P5, blood vessels harbor marked cells that originated from an E10.5 AdipoTrak+ source. These P30 RFP-labeled cells, which derive from the E10.5 AdipoTrak source, reside in the mural compartment (SMA+, PECAM−) of blood vessels and by P60 appear to evolve into RFP-marked adipocytes (Figures 6D and 6E). In the E10.5-P30 fate-mapping studies, the vast majority of adipocytes did not derive from adult progenitors; that is, they are LipidTox and Perilipin positive but RFP or lacZ negative, indicating that these adipocytes derived from the developmental progenitors as observed in our earlier fate-mapping studies (Figures 6E and S6H). In some instances, at P30, we did detect a few AdipoTrak-RFP-positive adipocytes located in juxtavascular positions, indicating that adult progenitor cell adipogenesis had begun (not shown). To see if additional adipocytes derive from the E10.5-marked cells, we examined depots after longer chase periods. At P60 and P120 chase points, we detected robust adipocyte marking with either the AdipoTrak RFP or lacZ reporter systems (Figure 6B-E), mirroring *SMA-Cre^{ERT2}* fate-mapping data (Figures 2 and 3). These AdipoTrak lineage-marked unilocular adipocytes coexpress Perilipin and are stained by LipidTox, indicating that E10.5 AdipoTrak-marked cells fate-map first into the adipose vasculature, acquire SMA expression, and then the marked adult progenitors differentiate into adipocytes (Figure 6E, bottom row). To confirm whether the E10.5 adult progenitors expresses *PPARγ* and *GFP*, we FACS-isolated GFP+ cells from E10.5 embryos and measured mRNA expression. We found that *PPARγ* and *GFP* were preferentially expressed in the AdipoTrak-marked cells compared to other embryonic cells (Figure S7A), supporting the notion that PPARγ and AdipoTrak are indeed expressed and that the AdipoTrak labeling system has high-fidelity marking, as previously reported (Tang et al., 2008, 2011; Zeve et al., 2012).

Adult AdipoTrak-Labeled Progenitors Are Required for Adult Adipose Tissue Homeostasis

The lineage-tracing data indicate that E10.5 AdipoTrak-labeled embryonic cells generate mural perivascular adult progenitors that are used in established/mature adult adipose depots, but not during adipose tissue development. To rigorously explore that notion and also the possibility that the E10.5 AdipoTrak-labeled cells are necessary for adult adipose tissue homeostasis, but not adipose tissue development, we again exploited the AdipoTrak-PPARγ genetic configuration. In these studies, we Dox suppressed AdipoTrak-PPARγ mice before conception (E0, control) or from E10.5 onward (only deleting PPARγ in the adult progenitor pool and not in developmental progenitors, mature adipocytes, etc.) and monitored adipose depot development at P30 or analyzed adult adipose tissue homeostasis over the subsequent 4 months (Figure 7A). The E10.5 + Dox AdipoTrak-PPARγ mice were born at appropriate Mendelian ratios, and pre- and postpartum studies indicated that the E10.5 AdipoTrak PPARγ deletion had no gross effect on tissue development (not shown). At P30, the E10.5 + Dox AdipoTrak-PPARγ mice had similar food intake, body weight, and fat content, although there might be a trend toward increased adiposity (Figures 7B, S7B, and S7C). Histological, molecular, and cell culture studies indicated that the P30 depots were relatively unaffected, with normal adipose depot architecture, normal levels of mature adipocyte markers, and normal adipogenic potential (Figures S7D–S7H). The P30 analyses indicate that mice in which AdipoTrak-PPARγ deletion was blocked by E10.5 and thereafter have apparently normal adipose depot development.

We continued to assess the E10.5 AdipoTrak-PPARγ cohort; over the ensuing months, we observed a decrease in fat content, while controls continued to increase fat mass (Figure 7B). By 5 months of age, the E10.5 AdipoTrak-PPARγ mice had approximately half the body fat as at P30 and were significantly leaner and had smaller adipose depots than 5-month-old littermate controls (Figures 7B–7D). Histological studies indicated that the mutants also had reduced adipocyte size; however, adipose depot architecture remained intact (Figure 7E). Even though these mice were lean and had small adipocytes (presumably derived from developmental progenitors), which are both typically associated with positive metabolic outcomes, the E10.5 + Dox AdipoTrak-PPARγ mice rather had metabolic dysfunctions often associated with dysfunctional obese or lipodystrophic adipocytes, glucose intolerance, and hypertriglyceridemia (Figures 7F and S7I). Expression analyses of adipose depots revealed reduced levels of mature adipocyte markers including PPARγ in the absence of changes in mural or endothelial cell marker expression (Figures 7G and 7H), resonating with our previous observations of SMA-PPARγ mutant mice (Figure 5). To evaluate potential cell-autonomous effects, we isolated SV cells from 5-month-old control and E10.5 + Dox AdipoTrak-PPARγ littermates. Although control SVF underwent adipogenesis and produced lipid-storing cells that expressed a host of adipocyte markers, the mutant SVF failed to differentiate (Figures 7I and

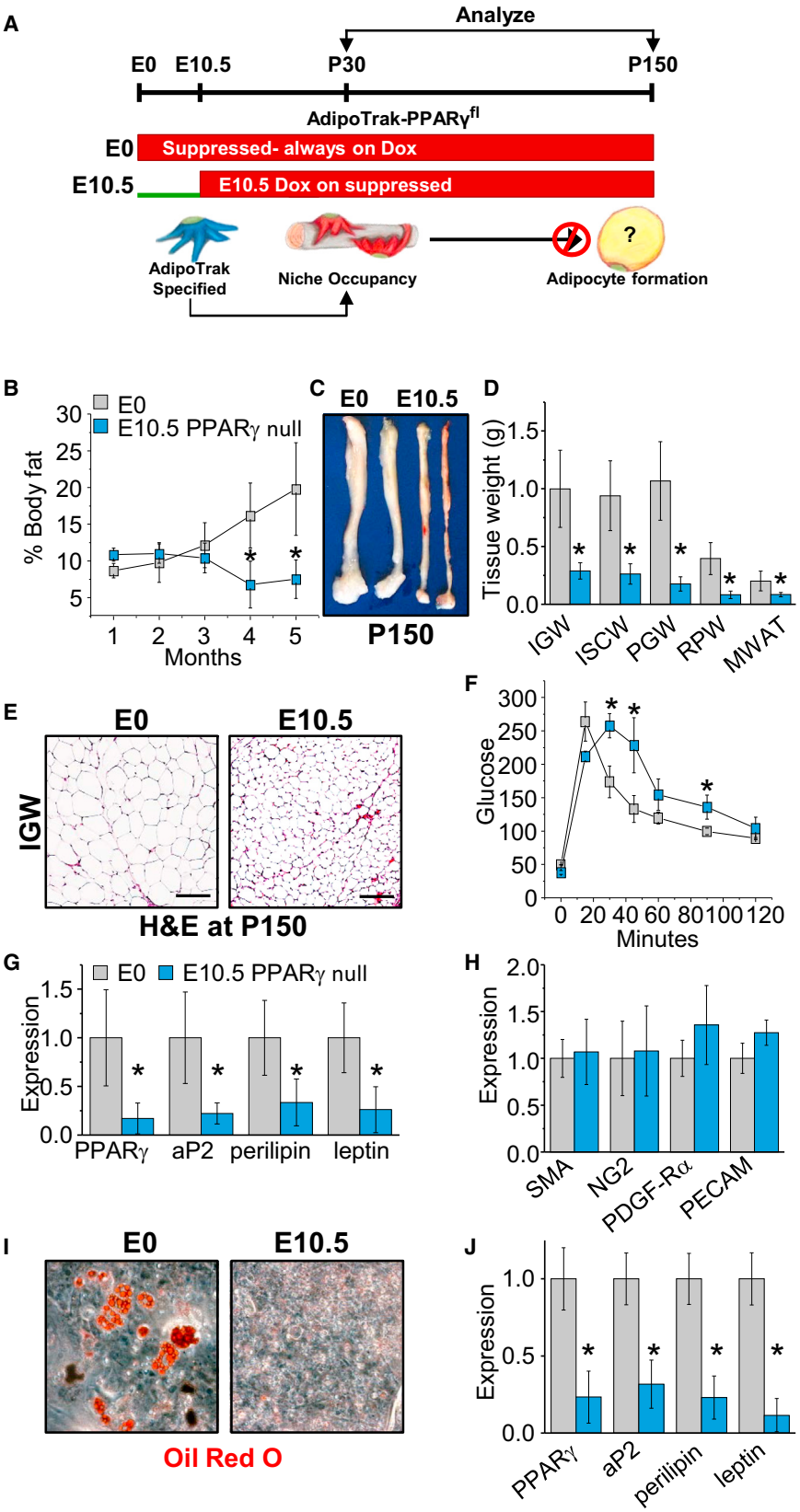

Figure 7. Adult Adipose Progenitors Are Essential for Adipose Depot Homeostasis and Maintenance

(A) Experimental design. AdipoTrak PPARγ$^{fl/tTA}$ mice were Dox suppressed prior to conception (E0 = control) or E10.5 and analyzed at P30 or P150 (5 months). Below: cartoon prediction, illustrating that adult adipose are specified and PPARγ deleted by E10.5 and fail to maintain adult adipose depots.

(B–E) AdipoTrak-PPARγ$^{fl/tTA}$ mice were Dox suppressed before conception (E0 = control) or from E10.5. Mice were maintained on Dox and analyzed at P150 (5 months of age) for body fat content (B), SQ depot size (C), tissue weights (D), and histology (E).

(F) Control and E10.5 Dox-suppressed AdipoTrak-PPARγ$^{fl/tTA}$ mice at 5 months (P150) of age were analyzed for glucose sensitivity by a glucose tolerance test.

(G and H) mRNA expression of mature adipocyte markers (G) or mural and endothelial cell markers (H) from SQ depots of control and E10.5 Dox-suppressed AdipoTrak-PPARγ$^{fl/tTA}$ mice.

(I and J) SV cells were isolated from 5-month-old control or E10.5 PPARγ deleted mice and cultured in adipogenic media and monitored for differentiation by oil red O staining (I) and mRNA expression of mature adipocyte markers (J). *p < 0.05 E10.5 PPARγ versus control (n = 4/group). Scale bar, 100 μm.

Data are expressed as mean ± SEM.

7J). These data support the E10.5 fate-mapping studies and indicate that deleting PPARγ in adult adipose progenitors before E10.5 results in normal adipose tissue development and function (at P30); however, adult adipose depots seem unable to properly maintain homeostasis, turnover, and metabolic control.

DISCUSSION

Several lines of evidence indicate that adipose stem cells are key elements for adipose depot formation, maintenance, and expansion in response to various stimuli (Berry et al., 2013; Gesta et al., 2007; Rodeheffer et al., 2008; Tang et al., 2008, 2011). Here, we combined fate-mapping methodologies and conditional blockade of adipocyte differentiation to investigate the adipose lineage and potential physiological contribution of adipose stem cells to depot development and/or maintenance. Our results indicate that there are two progenitor populations that give rise to adipocytes: developmental progenitors for adipose organogenesis and adult progenitors for adipose homeostasis. Both progenitor compartments express PPARγ and produce adipocytes yet have distinct functional and molecular properties and even reside in distinct anatomical niche localities. The two compartments also appear to arise from independent lineages and have distinct spatial and temporal patterns of specification. Both compartments are specified during embryogenesis, yet the adult progenitors appear to be marked even earlier than Developmental progenitors, even though they function later in adult adipose tissue homeostasis. Recent important studies by Hudak et al. (2014), using a novel Pref-1-GFP-dT transgenic cell killing strategy, support these notions and reinforce the idea of an early-formed (E10.5) adult compartment. The Pref-1-marked cells appear to overlap with those cells identified by the AdipoTrak fate-mapping tools. Yet the Pref-1 studies did not distinguish the temporal relationship of specification of the developmental and adult pools (Hudak et al., 2014). It is formally possible that developmental and adult progenitors share a proximate common, PPARγ (AdipoTrak)-negative, cellular origin that arises after node formation, streak elongation, germ-layer induction, and patterning. Such a putative cellular origin must then subsequently diverge and express PPARγ with quite different temporal, both embryonic and postnatal, and spatial patterns. Given the temporal proximity to somitogenesis, the spatial proximity to inductive signaling centers, and the quantity and pattern of appearance, we favor independent lineage derivation. However, additional studies, such as generating new fate-mapping models, are likely required. We do find that the E10.5 cells express both *PPARγ* and *GFP*, indicating that the reports have fidelity to endogenous expression and that molecular profiling might provide relevant targets for such new fate-mapping tools.

The notion of distinct progenitor compartments for organogenesis and homeostasis resonates with various other stem cell lineages such as neural, hematopoietic, and intestinal (Fordham et al., 2013; Li et al., 2013; Pietras and Passegué, 2013). In these lineages, stem cells that control either developmental or adult homeostasis have important molecular, anatomical, and functional differences and reside in different niche localities (Copley and Eaves, 2013; Knapp and Eaves, 2014; Pietras and Passegué, 2013). For example, some adult hematopoietic stem cells (HSCs) reside in a perivascular niche, but the two types of embryonic HSCs, primitive and developmental, do not (Copley and Eaves, 2013). Further, adult HSCs are also first specified early in embryogenesis, between E7.5 and E10.5, near the aorta-gonad-mesonepheros and placenta and eventually migrate and inhabit the adult bone marrow cavity, where they maintain and regenerate blood (Morrison and Scadden, 2014). The findings that various stem cell systems contain distinct developmental and adult stem compartments may hint at a general principle for organogenesis and homeostasis. It is also possible that distinct stem cell populations—proliferative developmental stem cells required for organogenic expansion and quiescent adult stem cells designed with preservation of the stem compartment as a key goal—may also be important to protect genomic integrity of the adult stem compartment. The two compartments may have distinct evolutionary history, which could account for the different attributes and timing and location of specification (López-Otín et al., 2013). The observation that during organogenesis, adipose depots are marked in an ordered temporal pattern, SQ organs first and Vis depots latter, supports the possibility that developmental progenitor compartments may themselves derive from different anlagen increasing developmental progenitor pool diversity, consistent with previous publications on adipocyte diversity (Berry and Rodeheffer, 2013; Lee et al., 2012; Sanchez-Gurmaches et al., 2012). Such independent stem compartments, developmental and adult, may generate cells geared to distinct functions; for instance, in the adipose system, developmental adipocytes may be designed with a focus on thermoregulation, while the adult lineage may be a bit more tuned to metabolic homeostasis.

Childhood and adult obesity may have unique attributes that could be accounted for by distinct adipose stem compartments. Human prospective and retrospective studies indicate that adipose mass and adipocyte number are primarily determined quite early in life, during embryogenesis and childhood (Cunningham et al., 2014; Dietz, 1997; Whitaker et al., 1997). This supports the possibility that developmental progenitors establish an adiposity set point, which is then fine-tuned by adult progenitors. Further studies aimed at manipulating developmental and adult stem cell number may help clarify the roles of the different progenitors in defining adiposity and adipocyte number.

Collectively, these data indicate that there are different functional attributes for adipose progenitor compartments during adipose tissue formation and homeostasis. The identification of the two types of adipose progenitor pools, of the transition of adult progenitors onto a perivascular position, and of their key roles in depot formation and maintenance may provide therapeutic entry points to address the epidemics of both childhood and adult obesity and the subsequent various negative metabolic derangements.

EXPERIMENTAL PROCEDURES

Animals

AdipoTrak (*PPARγ*^{tTA}; *TRE-H2B-GFP; TRE-Cre, R26R*^{lacZ}) mice were previously established in our lab (Tang et al., 2008, 2011; Zeve et al., 2012). *PPARγ* floxed allele and reporter lines *R26R*$^{RFP/lacZ}$ are available in The Jackson Laboratory. *SMA-Cre*^{ERT2} was generously provided by Dr. Pierre Chambon. Cre recombination was induced by administering TM dissolved in sunflower oil

(Sigma, 300 mg/kg intraperitoneal injection) on 2 consecutive days. Doxycycline (0.5 mg/ml in 1% sucrose) was provided in the drinking water and protected from light, and it was changed every 2–3 days. All animals were maintained under the guidelines of the U.T. Southwestern Medical Center Animal Care and Use Committee according to NIH guidelines under animal protocol 2010-0015.

Migration Assay

FACS-isolated GFP adipose stem cells were plated and grown to confluence. Once confluent, a scratch was made using a 200 μl pipette tip. Cells were washed three times with 1X PBS and photographed. Dulbecco's modified Eagle's medium (DMEM) supplemented with 10% fetal bovine serum (FBS) was added, and migration was monitored and photographed 8 hr later. Alternatively, FACS-isolated GFP− SV cells were plated in the bottom of a transwell dish and GFP+ adipose stem cells were plated in the upper chamber, and migration was monitored and photographed 12 hr later. Additionally, FACS-isolated GFP+ adipose stem cells were plated in the top of a transwell dish, and migration was monitored 12 hr later (Chen, 2005). Ten images were taken from each experimental parameter counted and averaged.

Adipose Explant Assay

Chopped (30–50 mg pieces) SQ fat depots (Gealekman et al., 2008) were washed 1X PBS. Pieces were encased in growth factor-free Matrigel (BD Bioscience). DMEM media supplemented with 10% FBS was added to the culture and outgrowths were photographed 7 days later. Progenitor cell occupancy was measured by counting the number of GFP+ cells/capillary sprouts/image after merging the fluorescence and phase images. A total of ten images from three explants from three individual mice were measured using Image J.

Statistical Analysis

Statistical significance was assessed by the two-tailed Student's t test. Error bars indicate SEM.

Additional methods are provided in the Supplemental Experimental Procedures.

SUPPLEMENTAL INFORMATION

Supplemental Information includes Supplemental Experimental Procedures and seven figures and can be found with this article online at http://dx.doi.org/10.1016/j.celrep.2014.09.049.

AUTHOR CONTRIBUTIONS

Y.J., D.C.B., and J.M.G. conceived, designed, and analyzed the experiments and wrote the manuscript. Y.J., D.C.B., and W.T. performed the experiments and analyzed the data. All authors discussed the results and commented on the manuscript.

ACKNOWLEDGMENTS

We are grateful to Dr. Luis Parada and the J.M.G. lab for use of equipment and helpful discussions. We thank Dr. Pierre Chambon for generously providing the SMA-Cre^{ERT2} mouse strain. This study was supported by the NIH and the National Institute of Diabetes and Digestive and Kidney Diseases grants (R01 DK066556, R01 DK064261, and R01 DK088220) to J.M.G. D.C.B. is supported by the National Heart, Blood and Lung Institute (5T32HL007360-34). Y.J. is supported by the American Heart Association (13POST14590008). J.M.G. is a cofounder and shareholder of Reata Pharmaceuticals.

Received: April 30, 2014
Revised: August 26, 2014
Accepted: September 24, 2014
Published: October 23, 2014

REFERENCES

Ahmadian, M., Suh, J.M., Hah, N., Liddle, C., Atkins, A.R., Downes, M., and Evans, R.M. (2013). PPARγ signaling and metabolism: the good, the bad and the future. Nat. Med. *19*, 557–566.

Ailhaud, G., Grimaldi, P., and Négrel, R. (1992). Cellular and molecular aspects of adipose tissue development. Annu. Rev. Nutr. *12*, 207–233.

Armulik, A., Genové, G., and Betsholtz, C. (2011). Pericytes: developmental, physiological, and pathological perspectives, problems, and promises. Dev. Cell *21*, 193–215.

Berry, R., and Rodeheffer, M.S. (2013). Characterization of the adipocyte cellular lineage in vivo. Nat. Cell Biol. *15*, 302–308.

Berry, D.C., Stenesen, D., Zeve, D., and Graff, J.M. (2013). The developmental origins of adipose tissue. Development *140*, 3939–3949.

Birsoy, K., Berry, R., Wang, T., Ceyhan, O., Tavazoie, S., Friedman, J.M., and Rodeheffer, M.S. (2011). Analysis of gene networks in white adipose tissue development reveals a role for ETS2 in adipogenesis. Development *138*, 4709–4719.

Cai, X., Lin, Y., Hauschka, P.V., and Grottkau, B.E. (2011). Adipose stem cells originate from perivascular cells. Biol. Cell *103*, 435–447.

Chawla, A., Schwarz, E.J., Dimaculangan, D.D., and Lazar, M.A. (1994). Peroxisome proliferator-activated receptor (PPAR) gamma: adipose-predominant expression and induction early in adipocyte differentiation. Endocrinology *135*, 798–800.

Chen, H.C. (2005). Boyden chamber assay. Methods Mol. Biol. *294*, 15–22.

Copley, M.R., and Eaves, C.J. (2013). Developmental changes in hematopoietic stem cell properties. Exp. Mol. Med. *45*, e55.

Crossno, J.T., Jr., Majka, S.M., Grazia, T., Gill, R.G., and Klemm, D.J. (2006). Rosiglitazone promotes development of a novel adipocyte population from bone marrow-derived circulating progenitor cells. J. Clin. Invest. *116*, 3220–3228.

Cunningham, S.A., Kramer, M.R., and Narayan, K.M. (2014). Incidence of childhood obesity in the United States. N. Engl. J. Med. *370*, 403–411.

Dani, C., Smith, A.G., Dessolin, S., Leroy, P., Staccini, L., Villageois, P., Darimont, C., and Ailhaud, G. (1997). Differentiation of embryonic stem cells into adipocytes in vitro. J. Cell Sci. *110*, 1279–1285.

Daniels, J. (2006). Obesity: America's epidemic. Am. J. Nurs. *106*, 40–49, quiz 49–50.

Dietz, W.H. (1997). Periods of risk in childhood for the development of adult obesity—what do we need to learn? J. Nutr. *127*, 1884S–1886S.

Duan, S.Z., Ivashchenko, C.Y., Whitesall, S.E., D'Alecy, L.G., Duquaine, D.C., Brosius, F.C., 3rd, Gonzalez, F.J., Vinson, C., Pierre, M.A., Milstone, D.S., and Mortensen, R.M. (2007). Hypotension, lipodystrophy, and insulin resistance in generalized PPARgamma-deficient mice rescued from embryonic lethality. J. Clin. Invest. *117*, 812–822.

Faust, I.M., Johnson, P.R., Stern, J.S., and Hirsch, J. (1978). Diet-induced adipocyte number increase in adult rats: a new model of obesity. Am. J. Physiol. *235*, E279–E286.

Fordham, R.P., Yui, S., Hannan, N.R., Soendergaard, C., Madgwick, A., Schweiger, P.J., Nielsen, O.H., Vallier, L., Pedersen, R.A., Nakamura, T., et al. (2013). Transplantation of expanded fetal intestinal progenitors contributes to colon regeneration after injury. Cell Stem Cell *13*, 734–744.

Gealekman, O., Burkart, A., Chouinard, M., Nicoloro, S.M., Straubhaar, J., and Corvera, S. (2008). Enhanced angiogenesis in obesity and in response to PPARgamma activators through adipocyte VEGF and ANGPTL4 production. Am. J. Physiol. Endocrinol. Metab. *295*, E1056–E1064.

Gesta, S., Tseng, Y.H., and Kahn, C.R. (2007). Developmental origin of fat: tracking obesity to its source. Cell *131*, 242–256.

Gupta, R.K., Arany, Z., Seale, P., Mepani, R.J., Ye, L., Conroe, H.M., Roby, Y.A., Kulaga, H., Reed, R.R., and Spiegelman, B.M. (2010). Transcriptional control of preadipocyte determination by Zfp423. Nature *464*, 619–623.

Gupta, R.K., Mepani, R.J., Kleiner, S., Lo, J.C., Khandekar, M.J., Cohen, P., Frontini, A., Bhowmick, D.C., Ye, L., Cinti, S., and Spiegelman, B.M. (2012). Zfp423 expression identifies committed preadipocytes and localizes to adipose endothelial and perivascular cells. Cell Metab. *15*, 230–239.

Han, J., Lee, J.E., Jin, J., Lim, J.S., Oh, N., Kim, K., Chang, S.I., Shibuya, M., Kim, H., and Koh, G.Y. (2011). The spatiotemporal development of adipose tissue. Development *138*, 5027–5037.

Hossain, P., Kawar, B., and El Nahas, M. (2007). Obesity and diabetes in the developing world—a growing challenge. N. Engl. J. Med. *356*, 213–215.

Hudak, C.S., Gulyaeva, O., Wang, Y., Park, S.M., Lee, L., Kang, C., and Sul, H.S. (2014). Pref-1 marks very early mesenchymal precursors required for adipose tissue development and expansion. Cell Reports *8*, 678–687.

Johnson, P.R., and Hirsch, J. (1972). Cellularity of adipose depots in six strains of genetically obese mice. J. Lipid Res. *13*, 2–11.

Kanda, T., Sullivan, K.F., and Wahl, G.M. (1998). Histone-GFP fusion protein enables sensitive analysis of chromosome dynamics in living mammalian cells. Curr. Biol. *8*, 377–385.

Knapp, D.J., and Eaves, C.J. (2014). Control of the hematopoietic stem cell state. Cell Res. *24*, 3–4.

Koh, Y.J., Kang, S., Lee, H.J., Choi, T.S., Lee, H.S., Cho, C.H., and Koh, G.Y. (2007). Bone marrow-derived circulating progenitor cells fail to transdifferentiate into adipocytes in adult adipose tissues in mice. J. Clin. Invest. *117*, 3684–3695.

Kopelman, P.G. (2000). Obesity as a medical problem. Nature *404*, 635–643.

Lee, Y.H., Petkova, A.P., Mottillo, E.P., and Granneman, J.G. (2012). In vivo identification of bipotential adipocyte progenitors recruited by β3-adrenoceptor activation and high-fat feeding. Cell Metab. *15*, 480–491.

Li, L., and Clevers, H. (2010). Coexistence of quiescent and active adult stem cells in mammals. Science *327*, 542–545.

Li, G., Fang, L., Fernández, G., and Pleasure, S.J. (2013). The ventral hippocampus is the embryonic origin for adult neural stem cells in the dentate gyrus. Neuron *78*, 658–672.

López-Otín, C., Blasco, M.A., Partridge, L., Serrano, M., and Kroemer, G. (2013). The hallmarks of aging. Cell *153*, 1194–1217.

Morrison, S.J., and Scadden, D.T. (2014). The bone marrow niche for haematopoietic stem cells. Nature *505*, 327–334.

Nehls, V., and Drenckhahn, D. (1993). The versatility of microvascular pericytes: from mesenchyme to smooth muscle? Histochemistry *99*, 1–12.

Pietras, E.M., and Passegué, E. (2013). Linking HSCs to their youth. Nat. Cell Biol. *15*, 885–887.

Prins, J.B., and O'Rahilly, S. (1997). Regulation of adipose cell number in man. Clin. Sci. *92*, 3–11.

Rigamonti, A., Brennand, K., Lau, F., and Cowan, C.A. (2011). Rapid cellular turnover in adipose tissue. PLoS ONE *6*, e17637.

Rodeheffer, M.S., Birsoy, K., and Friedman, J.M. (2008). Identification of white adipocyte progenitor cells in vivo. Cell *135*, 240–249.

Rosen, E.D., and Spiegelman, B.M. (2006). Adipocytes as regulators of energy balance and glucose homeostasis. Nature *444*, 847–853.

Rosen, E.D., Sarraf, P., Troy, A.E., Bradwin, G., Moore, K., Milstone, D.S., Spiegelman, B.M., and Mortensen, R.M. (1999). PPAR gamma is required for the differentiation of adipose tissue in vivo and in vitro. Mol. Cell *4*, 611–617.

Rousseau, K., Atcha, Z., and Loudon, A.S. (2003). Leptin and seasonal mammals. J. Neuroendocrinol. *15*, 409–414.

Sanchez-Gurmaches, J., Hung, C.M., Sparks, C.A., Tang, Y., Li, H., and Guertin, D.A. (2012). PTEN loss in the Myf5 lineage redistributes body fat and reveals subsets of white adipocytes that arise from Myf5 precursors. Cell Metab. *16*, 348–362.

Schwimmer, H., and Haim, A. (2009). Physiological adaptations of small mammals to desert ecosystems. Integr. Zool. *4*, 357–366.

Spalding, K.L., Arner, E., Westermark, P.O., Bernard, S., Buchholz, B.A., Bergmann, O., Blomqvist, L., Hoffstedt, J., Näslund, E., Britton, T., et al. (2008). Dynamics of fat cell turnover in humans. Nature *453*, 783–787.

Spiegelman, B.M., and Flier, J.S. (2001). Obesity and the regulation of energy balance. Cell *104*, 531–543.

Tang, W., Zeve, D., Suh, J.M., Bosnakovski, D., Kyba, M., Hammer, R.E., Tallquist, M.D., and Graff, J.M. (2008). White fat progenitor cells reside in the adipose vasculature. Science *322*, 583–586.

Tang, W., Zeve, D., Seo, J., Jo, A.Y., and Graff, J.M. (2011). Thiazolidinediones regulate adipose lineage dynamics. Cell Metab. *14*, 116–122.

Tontonoz, P., and Spiegelman, B.M. (2008). Fat and beyond: the diverse biology of PPARgamma. Annu. Rev. Biochem. *77*, 289–312.

Tontonoz, P., Hu, E., and Spiegelman, B.M. (1994). Stimulation of adipogenesis in fibroblasts by PPAR gamma 2, a lipid-activated transcription factor. Cell *79*, 1147–1156.

Tran, K.V., Gealekman, O., Frontini, A., Zingaretti, M.C., Morroni, M., Giordano, A., Smorlesi, A., Perugini, J., De Matteis, R., Sbarbati, A., et al. (2012). The vascular endothelium of the adipose tissue gives rise to both white and brown fat cells. Cell Metab. *15*, 222–229.

Weissman, I.L. (2000). Stem cells: units of development, units of regeneration, and units in evolution. Cell *100*, 157–168.

Wendling, O., Bornert, J.M., Chambon, P., and Metzger, D. (2009). Efficient temporally-controlled targeted mutagenesis in smooth muscle cells of the adult mouse. Genesis *47*, 14–18.

Whitaker, R.C., Wright, J.A., Pepe, M.S., Seidel, K.D., and Dietz, W.H. (1997). Predicting obesity in young adulthood from childhood and parental obesity. N. Engl. J. Med. *337*, 869–873.

Zeve, D., Seo, J., Suh, J.M., Stenesen, D., Tang, W., Berglund, E.D., Wan, Y., Williams, L.J., Lim, A., Martinez, M.J., et al. (2012). Wnt signaling activation in adipose progenitors promotes insulin-independent muscle glucose uptake. Cell Metab. *15*, 492–504.